G-Quadruplexes

International Edition: DOI: 10.1002/anie.201507569
German Edition: DOI: 10.1002/ange.201507569

Reversible pH Switch of Two-Quartet G-Quadruplexes Formed by Human Telomere

Petra Galer, Baifan Wang, Primož Šket, and Janez Plavec**

Abstract: *A four-repeat human telomere DNA sequence without the 3′-end guanine, d[TAGGG(TTAGGG)$_2$TTAGG] (htel1-ΔG23) has been found to adopt two distinct two G-quartet antiparallel basket-type G-quadruplexes, TD and KDH$^+$ in presence of KCl. NMR, CD, and UV spectroscopy have demonstrated that topology of KDH$^+$ form is distinctive with unique protonated T18·A20$^+$·G5 base triple and other capping structural elements that provide novel insight into structural polymorphism and heterogeneity of G-quadruplexes in general. Specific stacking interactions amongst two G-quartets flanking base triples and base pairs in TD and KDH$^+$ forms are reflected in 10 K higher thermal stability of KDH$^+$. Populations of TD and KDH$^+$ forms are controlled by pH. The (de)protonation of A20 is the key for pH driven structural transformation of htel1-ΔG23. Reversibility offers possibilities for its utilization as a conformational switch within different compartments of living cell enabling specific ligand and protein interactions.*

Guanine-rich DNA sequences can fold into G-quadruplexes in the presence of cations, such as K^+, Na^+, or NH_4^+. G-quadruplex contains several planar G-quartets which comprise of four guanines connected by Hoogsteen hydrogen bonds, and are further stabilized by cations located at the center of G-quartets.[1] G-rich sequences found in human genome including hexanucleotide repeat TTAGGG in telomeres are capable to fold into G-quadruplexes, which are promising targets for anticancer drug development.[2] Owing to their special four G-strand architectures and sensibility to cations and ligand binding, G-quadruplexes have been applied to DNA nanotechnology, DNAzymes and design of biosensors.[3] Recently, pH has been utilized to regulate formation and conformational transitions of G-quadruplexes.[4]

Human telomere G-rich sequences have been shown to fold into diverse topologies in the presence of different cations, heterocyclic ligands, solution environments, and flanking sequences.[5] For instance, human telomere sequence d[TAGGG(TTAGGG)$_3$] (designated as *htel1*) in the presence of K^+ ions predominantly folds into hybrid-1 type G-quadruplex containing three G-quartets that are connected by one propeller and two lateral loops.[5a–c] A related sequence derived from human telomere repeat, d[GGG(TTAGGG)$_3$T], forms intramolecular antiparallel basket-type G-quadruplex with only two G-quartets in K^+ ion solution.[5e,f] The two G-quartet basket-type topology was suggested to represent an intermediate in interconversion amongst hybrid type telomere G-quadruplexes.[5e] Furthermore, folding of G-quadruplex structures most likely proceeds through numerous intermediates as has been proposed by several groups.[5e,j,6] Chaires and co-workers proposed that an early step in the folding pathway of the human telomere DNA is formation of an antiparallel intermediate with either a chair or basket-type topology.[6b] Recently, two G-quartet antiparallel basket-type topology has been identified under "essentially physiological conditions".[7] Owing to a great role suggested for G-quadruplexes with antiparallel basket-type topology, sequence d[TAGGG(TTAGGG)$_2$TTAGG] (designated as *htel1-ΔG23*), which is a truncated version of the human telomere sequence forming hybrid-1 G-quadruplex, has been examined by NMR, CD, and UV spectroscopy. Formal deletion of the 3′-end guanine residue from *htel1* was expected to result in antiparallel G-quadruplex with only two G-quartets and consequently three extra-quartet guanine residues being involved in connecting loops in the presence of K^+ ions. At the outset, however, intriguing dynamic conformational equilibrium has been observed upon variation of pH.

htel1-ΔG23 was folded into G-quadruplex structures upon titration of K^+ ions up to 100 mM concentration at 298 K and neutral pH. As shown in Figure 1a, the δ 10.4–12.1 ppm region of 1D ^{1}H NMR spectrum indicated formation of G-quadruplex consisting of two G-quartets at 5 mM concentration of K^+ ions. Unambiguous assignment was achieved by synthesis of residue specific partially (8%) ^{15}N, ^{13}C-isotopically labeled oligonucleotides (Supporting Information, Figure S1). Characteristics of ^{1}H and ^{15}N-edited ^{1}H NMR spectra suggested coexistence of a G-quadruplex (named as TD) in addition to partially folded (named as KD) and unfolded *htel1-ΔG23* at 5 mM K^+ ion concentration (Figure 1a). Under this condition, the relative populations of TD, KD, and unfolded forms were 30:15:55, respectively. Signals for all guanine imino protons except for G5 and G11 of TD form were observed in ^{1}H NMR spectrum at 5 mM K^+ solution. On the other hand, resolved guanine imino protons were observed only for G4, G10, G11 and G15 of KD (marked

[*] Dr. P. Galer, Dr. B. Wang, Dr. P. Šket, Prof. Dr. J. Plavec
Slovenian NMR Center, National Institute of Chemistry
Hajdrihova 19, Ljubljana (Slovenia)
Dr. P. Šket, Prof. Dr. J. Plavec
EN-FIST Center of Excellence
Trg OF 13, 1000 Ljubljana (Slovenia)
Prof. Dr. J. Plavec
Faculty of Chemistry and Chemical Technology, University of Ljubljana
Večna pot 113, Ljubljana (Slovenia)
E-mail: primoz.sket@ki.si
janez.plavec@ki.si

Supporting information for this article is available on the WWW under http://dx.doi.org/10.1002/anie.201507569.

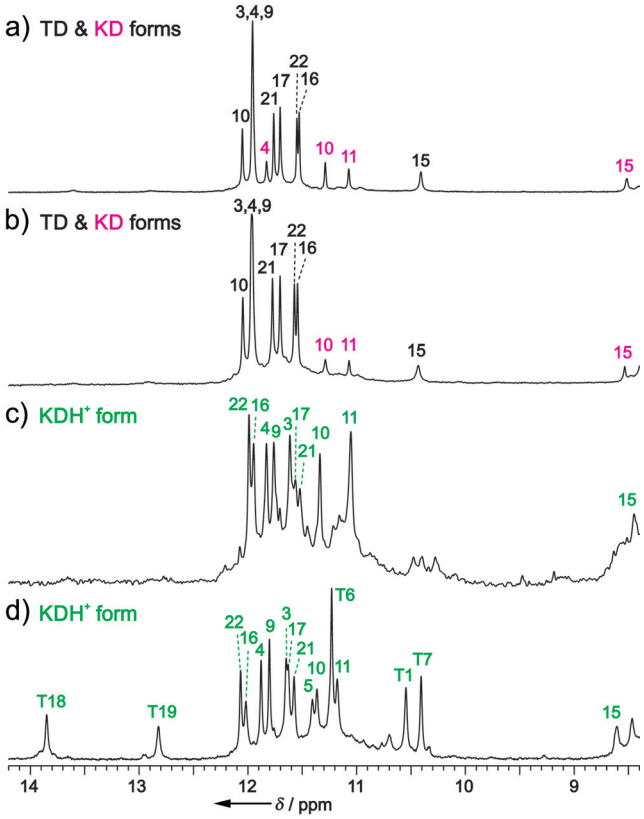

Figure 1. Imino region of ^{1}H NMR spectra of *htel1-ΔG23* at a) 5 mM KCl, pH 7.0, 298 K, b) 70 mM KCl, pH 7.0, 298 K, c) 70 mM KCl, pH 5.0, 298 K, and d) 70 mM KCl, pH 5.0, 278 K. Oligonucleotide concentration 1.0 mM. Resonance signals of TD, KD, and KDH$^+$ forms are marked with black, magenta, and green, respectively.

with magenta in Figure 1 a) suggesting that G-quartets are not formed completely. It is interesting to note that imino signal for G15 of KD exhibits upfield chemical shift of δ 8.52 ppm, which suggests its unusual hydrogen bonding pattern. Upon increasing concentration of K^+ ions to 70 mM, population of TD increased by 42 unit %, while population of KD remained practically unchanged (TD/KD/unfolded = 72:19:9, Figure 1 b). The same TD/KD/unfolded ratio was observed already at 30 mM KCl, where steady-state conditions were reached (Supporting Information, Figure S2). Various experimental conditions were further evaluated for their influence on relative ratio of TD and KD forms in solution. Observing populations of different forms during titrations suggested that formation of TD is thermodynamically, while folding into KD is kinetically controlled. Population of KD form significantly increased by lowering pH to 5.0 and dominated at 278 K (Figures 1 c,d). Conversion from one form to another is fast on NMR time scale and occurs immediately after changing pH and acquiring NMR spectrum (dead time ca. 3 minutes). The observed signals for guanine imino protons indicated formation of a new G-quadruplex structure, further marked as KDH$^+$. It is interesting to note that signals of imino protons of G4, G10, G11 and G15 exhibited a small chemical shift change with respect to KD form upon lowering pH to 5.0 (Figure 1). Partial assignment of NOESY cross-peaks of KD (Supporting Information, Figure S3) together with other NMR data and considering its low population suggest that KD form can be considered as a pre-folded state on the way to KDH$^+$. NMR signals of imino protons of T1, T6, T7, T18, and T19 were observed for KDH$^+$ form. Their chemical shifts indicated that T18 and T19 are involved in A·T base pairs (Figure 1 d). Imino protons of G15 in TD, KD, and KDH$^+$ forms exhibit broader linewidths and more effective T_2 relaxation with respect to other imino protons suggesting their exposure to solvent exchange in a system that involves dynamic structure interconversions.

The monomeric nature of both TD and KDH$^+$ forms was inferred from translation diffusion coefficients of $(1.40 \pm 0.05) \times 10^{-6}$ cm^{2}s^{-1} at 298 K.[8] Antiparallel topologies of both TD and KDH$^+$ forms were suggested from CD spectra that showed positive bands around 295 and 248 nm and negative band around 264 nm (Supporting Information, Figure S4).

A perusal of the aromatic-anomeric region of 2D NOESY spectra of TD and KDH$^+$ forms at 70 mM concentration of K^+ ions showed strong intraresidual cross-peaks for G3, G9, G16, and G21, indicating preference for *syn* conformation across their glycosidic bonds (Figure 2; Supporting Information,

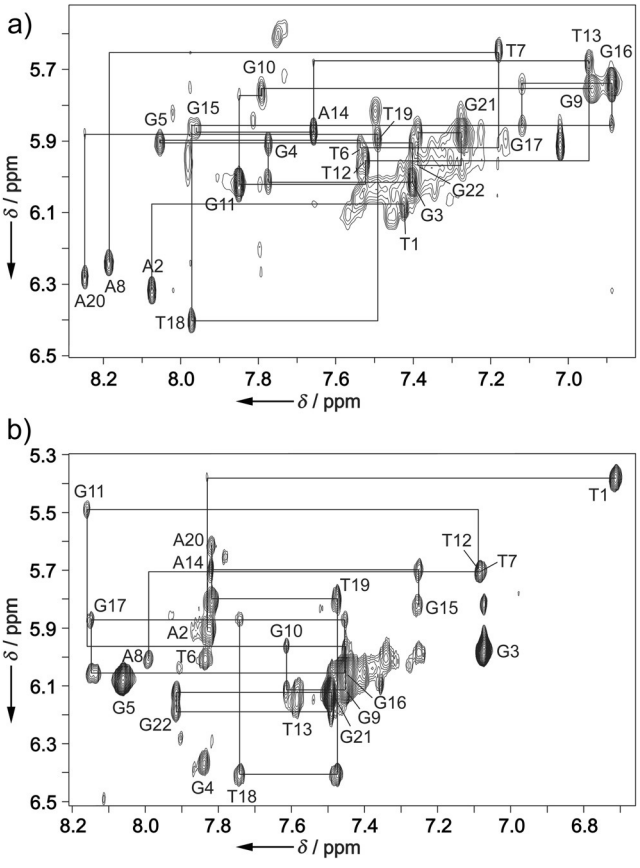

Figure 2. Aromatic-anomeric region of NOESY spectra of *htel1-ΔG23* in the presence of 70 mM KCl at a) pH 7.0, 298 K, b) pH 5.0, 278 K in 10% D_2O. Mixing times were 200 ms in (a) and 150 ms in (b). Sequential H8/H6-H1′ connectivities for T1-A2, G3-A8, G9-G15, G16-A20, and G21-G22 segments of TD (a) and for T1-A2, T7-A8, G9-T12, A14-G15, G16-A20, and G21-G22 segments of KDH$^+$ (b) are labeled by solid lines.

Figure S5). Furthermore, G11 in TD and G5 in KDH$^+$ also adopt *syn* glycosidic conformations.

NOE cross-peaks between imino and H8 protons were consistent with formation of G10→G3→G16→G22 and G17→G4→G9→G21 quartets in TD form (arrows indicate imino-H8 cross-peaks around each G-quartet, connectivities between the last and the first residues in both G-quartets are implied; Supporting Information, Figure S6). The glycosidic conformations of guanines are in *syn-syn-anti-anti* arrangements for both G-quartets in TD form. Identification of G-quartets has enabled us to propose antiparallel basket-type topology for TD (Figure 3a). The upper and lower G-quartets

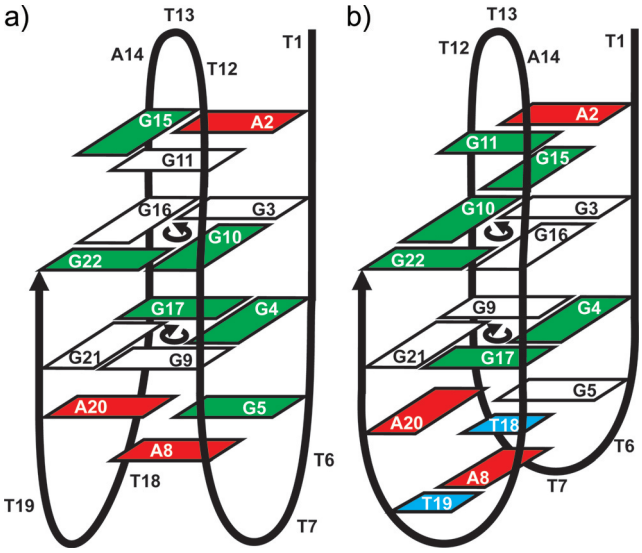

Figure 3. Topologies of a) TD and b) KDH$^+$ forms. Guanines in *syn* and *anti* conformations are colored white and green, respectively, adenines are red, and thymines are blue. Note that residue A20 is protonated in the KDH$^+$ form. Anticlockwise and clockwise directionalities of hydrogen bonds within G-quartets are marked.

exhibit anticlockwise and clockwise directionalities of hydrogen bonds, respectively. Strands and loops in TD structures progress in −ld + l arrangements.[9] In KDH$^+$ form, the G10→G22→G16→G3 and G17→G21→G9→G4 quartets were identified (Supporting Information, Figure S6). Hence, KDH$^+$ form has the same basket-type topology as TD form but with a + ld−l loop progression (Figure 3b). It is interesting to note that in KDH$^+$ and TD forms the upper and lower G-quartets exhibit the same directionalities of hydrogen bonds. However, the actual donor→acceptor directionalities of a given guanine residue are different. For example, G22 is donor and G10 is acceptor of Hoogsteen type hydrogen bonds in TD form, whereas G10 is donor and G22 is acceptor of hydrogen bonds in KDH$^+$ form (Supporting Information, Figure S7). Altogether, topologies of TD and KDH$^+$ forms exhibit the same inherent polarity of consecutive strands, which are in perfect agreement with identical shapes of their CD spectra (Supporting Information, Figure S4). Of note, CD signatures of both TD and KDH$^+$ are of the right-handed G-quadruplexes.

Comparative chemical shift analysis of TD and KDH$^+$ forms established the protonation site of the latter at A20 N1 (Figure 4). In the KDH$^+$ form, C2 and H2 chemical shifts of A20 (δ_{13C} 148.0 ppm, δ_{1H} 7.82 ppm) and A8 (δ_{13C} 152.8 ppm,

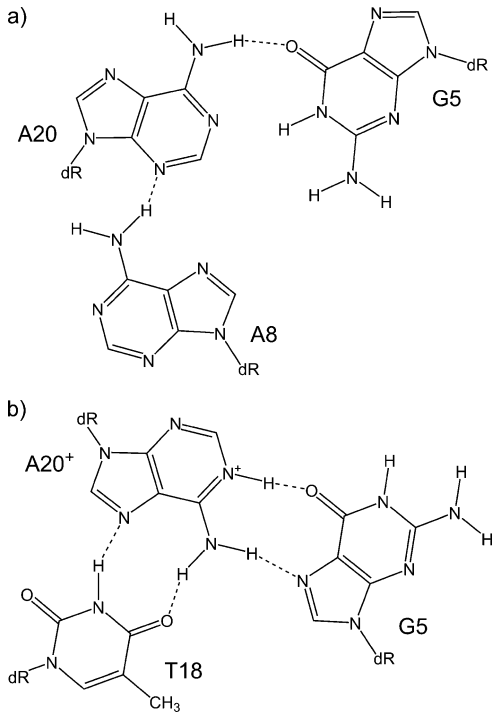

Figure 4. Representations of the A8·A20·G5 and T18·A20$^+$·G5 base triples in structures of a) TD and b) KDH$^+$ forms. Dashed lines illustrate hydrogen bonding established with observation of imino and amino protons in NMR spectra.

δ_{1H} 6.30 ppm) are unique spectral markers of non-protonated A8 that is stacked on A20 protonated at N1 (cf. Figures 3b and 4b).[10] Reference chemical shifts of A20 (δ_{13C} 156.0 ppm, δ_{1H} 8.38 ppm) and A8 (δ_{13C} 154.7 ppm, δ_{1H} 7.98 ppm) in TD form are distinctly different.

Preliminary molecular modelling of TD indicated that A2·G15·G11 and A8·A20·G5 base triples are stacked on the upper and lower G-quartets, respectively (Figure 3a; Supporting Information, Figure S8). While formation of A8·A20·G5 base triple is not supported by mutual NOE contacts amongst imino and aromatic protons of the three residues, they are well positioned through observation of several NOEs between the protons of G17→G4→G9→G21 quartet and individual residues of this base triple (Supporting Information, Figure S9). In the KDH$^+$ form, G11 is involved in G·G N1-carbonyl base pair with G15, which is sandwiched between the upper G-quartet and A2 (Figure 3b; Supporting Information, Figures S8 and S10). In the lower part of the KDH$^+$ structure, G17→G21→G9→G4 quartet is flanked by T18·A20$^+$·G5 base triple, which is stacked further with T19·A8 base pair (Figure 3b; Supporting Information, Figures S6 and S8). The above observations are fully consistent with earlier studies showing that human telomere two-G-quartet G-quadruplexes are stabilized by the extensive stacking of base triples and base pairs.[5e,f]

Variation of pH at 298 K shifts relative populations of TD and KDH$^+$ forms of *htel1-ΔG23* (Figure 5). During the pH lowering step from neutral to pH 5.0, population of TD decreased by 62 unit %, while at the same time population of

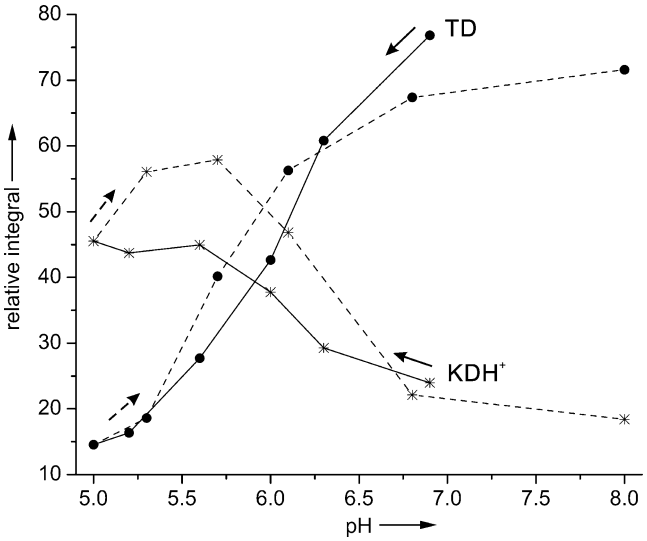

Figure 5. Populations of TD and KDH$^+$ forms as a function of pH at 298 K. Titration started from pH 6.9, which was lowered to 5.0 (——), and continued from 5.0 to 8.0 (-----). Relative integral (±3 unit %) corresponding to percentage of TD and KDH$^+$ forms was determined by integration of ^{1}H NMR signal at δ 6.89 ppm (G16 H8 of TD form, ●) and at δ 6.67 ppm (T1 H6 of KDH$^+$ form, ⋆).

KDH$^+$ form increased by 22 unit %. In the subsequent step, when pH was increased from 5.0 to 8.0, population of TD increased by 57 unit %, while population of KDH$^+$ form decreased by 27 unit % (Figure 5; Supporting Information, Figure S11). Analysis of population changes as a function of pH indicated a mid-transitional pH between 5.8 and 6.3. Lowering and increasing pH cycles controlling interconversions between TD and KDH$^+$ forms were repeated 9 times.

Apparent melting temperatures of TD and KDH$^+$ forms as determined by UV melting experiments were 319 and 329 K, respectively (Supporting Information, Figure S12). Interpretation of values determined under different experimental conditions should be performed with great caution. Nevertheless, the base pairs and base triples and their effective stacking interactions, especially of the T18·A20$^+$·G5 base triple, could be crucial for higher thermal stability of KDH$^+$ form under low pH. As a drop and an increase of populations of TD and KDH$^+$ forms are not the same upon lowering pH from neutral to 5.0, respectively, there must be additional form(s) involved in the process that could not be identified at this stage. However, lowering of pH leads to A20 N1 protonation, which shifts equilibrium due to stabilization of KDH$^+$ form and drives the reversible structure transformation. Comparison with alternative pH-driven nanoswitches utilizing i-motif formation[11] demonstrates similar transition pH values as observed for *htel1-ΔG23* G-quadruplexes.

In conclusion, we have found that *htel1-ΔG23* in the presence of KCl forms two distinct two G-quartet antiparallel basket-type G-quadruplexes. The topology of the KDH$^+$ form exhibits unique structural features including orientations of loops and capping base pairs and base triple that effectively stack on two-quartet core. Its topology is thus distinctive to any reported human telomere G-quadruplexes with unique protonated T18·A20$^+$·G5 base triple. A protonation–deprotonation equilibrium controlling reversible TD-KDH$^+$ transformations is a conformational switch that could provide a platform for further design of pH switches in more elaborated bio-nanostructures, such as molecular motors.

Acknowledgements

This work was supported by the Slovenian Research Agency (ARRS, grants P1-0242 and J1-6733).

Keywords: DNA · G-quadruplexes · human telomere repeat · NMR spectroscopy · topology

How to cite: *Angew. Chem. Int. Ed.* **2016**, *55*, 1993–1997
Angew. Chem. **2016**, *128*, 2033–2037

[1] a) M. Gellert, M. N. Lipsett, D. R. Davies, *Proc. Natl. Acad. Sci. USA* **1962**, *48*, 2013–2018; b) D. Sen, W. Gilbert, *Nature* **1988**, *334*, 364–366; c) *Biological Relevance & Therapeutic Applications of DNA- & RNA-Quadruplexes* (Ed.: D. Monchaud), Future Science, London, **2015**.

[2] a) S. M. Kerwin, *Curr. Pharm. Des.* **2000**, *6*, 441–471; b) S. Neidle, *FEBS J.* **2010**, *277*, 1118–1125; c) S. Balasubramanian, L. H. Hurley, S. Neidle, *Nat. Rev. Drug Discovery* **2011**, *10*, 261–275; d) A. Bugaut, S. Balasubramanian, *Nucleic Acids Res.* **2012**, *40*, 4727–4741; e) E. Y. N. Lam, D. Beraldi, D. Tannahill, S. Balasubramanian, *Nat. Commun.* **2013**, *4*, 1796; f) S. A. Ohnmacht, S. Neidle, *Bioorg. Med. Chem. Lett.* **2014**, *24*, 2602–2612; g) G. W. Collie, N. H. Campbell, S. Neidle, *Nucleic Acids Res.* **2015**, *43*, 4785–4799.

[3] a) L. A. Yatsunyk, O. Mendoza, J. L. Mergny, *Acc. Chem. Res.* **2014**, *47*, 1836–1844; b) J. L. Neo, K. Kamaladasan, M. Uttamchandani, *Curr. Pharm. Des.* **2012**, *18*, 2048–2057; c) F. Wang, X. Liu, I. Willner, *Angew. Chem. Int. Ed.* **2015**, *54*, 1098–1129; *Angew. Chem.* **2015**, *127*, 1112–1144.

[4] Y. Yan, J. Tan, Y. Lu, S. Yan, K. Wong, D. Li, L. Gu, Z. Huang, *Biochim. Biophys. Acta Gen. Subj.* **2013**, *1830*, 4935–4942.

[5] a) K. N. Luu, A. T. Phan, V. Kuryavyi, L. Lacroix, D. J. Patel, *J. Am. Chem. Soc.* **2006**, *128*, 9963–9970; b) J. Dai, C. Punchihewa, A. Ambrus, D. Chen, R. A. Jones, D. Yang, *Nucleic Acids Res.* **2007**, *35*, 2440–2450; c) A. T. Phan, V. Kuryavyi, K. N. Luu, D. J. Patel, *Nucleic Acids Res.* **2007**, *35*, 6517–6525; d) J. Dai, M. Carver, C. Punchihewa, R. A. Jones, D. Yang, *Nucleic Acids Res.* **2007**, *35*, 4927–4940; e) Z. Zhang, J. Dai, E. Veliath, R. A. Jones, D. Yang, *Nucleic Acids Res.* **2010**, *38*, 1009–1021; f) K. W. Lim, S. Amrane, S. Bouaziz, W. Xu, Y. Mu, D. J. Patel, K. N. Luu, A. T. Phan, *J. Am. Chem. Soc.* **2009**, *131*, 4301–4309; g) B. Heddi, A. T. Phan, *J. Am. Chem. Soc.* **2011**, *133*, 9824–9833; h) G. N. Parkinson, M. P. H. Lee, S. Neidle, *Nature* **2002**, *417*, 876–880; i) Y. Wang, D. J. Patel, *Structure* **1993**, *1*, 263–282; j) T. Mashimo, H. Sugiyama, *Nucleic Acids Symp. Ser.* **2007**, *51*, 239–240.

[6] a) P. Stadlbauer, L. Trantírek, T. E. Cheatham, J. Koča, J. Šponer, *Biochimie* **2014**, *105*, 22–35; b) R. D. Gray, J. O. Trent, J. B. Chaires, *J. Mol. Biol.* **2014**, *426*, 1629–1650; c) A. Ambrus, D. Chen, J. Dai, T. Bialis, R. A. Jones, D. Yang, *Nucleic Acids Res.* **2006**, *34*, 2723–2735; d) T. Mashimo, H. Yagi, Y. Sannohe, A.

Rajendran, H. Sugiyama, *J. Am. Chem. Soc.* **2010**, *132*, 14910 – 14918; e) S. Čeru, P. Šket, I. Prislan, J. Lah, J. Plavec, *Angew. Chem. Int. Ed.* **2014**, *53*, 4881 – 4884; *Angew. Chem.* **2014**, *126*, 4981 – 4984; f) I. Bessi, H. R. A. Jonker, C. Richter, H. Schwalbe, *Angew. Chem. Int. Ed.* **2015**, *54*, 8444 – 8448; *Angew. Chem.* **2015**, *127*, 8564 – 8568.

[7] R. Hänsel, F. Löhr, L. Trantirek, V. Dötsch, *J. Am. Chem. Soc.* **2013**, *135*, 2816 – 2824.

[8] a) M. Trajkovski, P. Šket, J. Plavec, *Org. Biomol. Chem.* **2009**, *7*, 4677 – 4684; b) M. Marušič, P. Šket, L. Bauer, V. Viglasky, J. Plavec, *Nucleic Acids Res.* **2012**, *40*, 6946 – 6956; c) M. Trajkovski, M. Webba da Silva, J. Plavec, *J. Am. Chem. Soc.* **2012**, *134*, 4132 – 4141; d) M. Cevec, J. Plavec, *Biochemistry* **2005**, *44*, 15238 – 15246.

[9] M. Webba da Silva, *Chem. Eur. J.* **2007**, *13*, 9738 – 9745.

[10] a) P. Legault, A. Pardi, *J. Am. Chem. Soc.* **1994**, *116*, 8390 – 8391; b) R. Stefl, F. C. Oberstrass, J. L. Hood, M. Jourdan, M. Zimmermann, L. Skrisovska, C. Maris, L. Peng, C. Hofr, R. B. Emeson, F. H. T. Allain, *Cell* **2010**, *143*, 225 – 237; c) P. Šponková, S. Foldynová-Trantírková, K. Bednářová, R. Fiala, M. Vorlíčková, L. Trantírek, *Nucleic Acids Res.* **2015**, *43*, 4733 – 4745.

[11] a) Y. P. Bhaysar-Jog, E. Van Dornshuld, T. A. Brooks, G. S. Tschumper, R. M. Wadkins, *Biochemistry* **2014**, *53*, 1586 – 1594; b) L. Lannes, S. Halder, Y. Krishnan, H. Schwalbe, *ChemBioChem* **2015**, *16*, 1647 – 1656; c) Y. Ding, A. M. Fleming, L. He, C. J. Burrows, *J. Am. Chem. Soc.* **2015**, *137*, 9053 – 9060.

Received: August 13, 2015
Revised: November 4, 2015
Published online: January 6, 2016

